PHYSICAL REVIEW B VOLUME 37, NUMBER 3 15 JANUARY 1988-II

Virtual-bound-state effects in core-level spectra of light rare-earth alloys

J. C. Fuggle
Research Institute for Materials, Faculty of Science, University of Nijmegen,
Toernooiveld, 6525 ED Nijmegen, The Netherlands

O. Gunnarsson
Max-Planck-Institut für Festkörperforschung, D-7000 Stuttgart 80,
Federal Republic of Germany

G. A. Sawatzky
Materials Science Center, State University of Groningen, Nijenborgh 16,
9747 AG Groningen, The Netherlands

K. Schönhammer
Institut für Theoretische Physik, Universität Göttingen, D-3400 Göttingen,
Federal Republic of Germany

(Received 19 August 1986; revised manuscript received 27 May 1987)

We document observations of unusual distortion of the individual component core-level line shapes of x-ray photoemission peaks in alloys of the light rare earths. We show, by a rather simple treatment, that this distortion is a result of hybridization of the $4f$ levels with valence states in the final state and that it is diagnostic of the strength of such hybridization.

I. INTRODUCTION

It is by now well recognized that the $4f$ levels of Ce and the early rare earths are significantly hybridized with the conduction states. (See, e.g., Refs. 1–12.) Nevertheless this conclusion is strongly based on studies of the intensities of the components of x-ray photoemission (XPS) core lines[1–3,8–12] and hence relies on a rather complicated theoretical description and simplifying assumptions concerning the core hole potential. It is not as widely recognized that the line shapes of individual components of the early rare-earth XPS core-level spectra can be considerably distorted if their relative energy separations correspond to a region with structure in the density of occupied valence states with respect to the Fermi level (E_F), and provided there is hybridization of the $4f$ levels with these valence states. In this paper we display such distorted line shapes and explain them in terms of the interaction of discrete f states with structured continua. We will show that the component line shapes can, in principle, be used to obtain information on the importance of hybridization, using rather simple arguments. We will also discuss the relationship of this distortion of core line shapes, previously observed in adsorbates,[13–16] to related effects in other spectroscopies such as ultraviolet and (resonance) valence-band photoemission, and Auger and x-ray absorption spectroscopies.

The physics of the effect[17] in core-level spectroscopies is the same as the virtual-bound-state broadening for impurity states in metals[18–21] and impurity Auger line shapes[20–25] and can be understood using the example of the $3d$ XPS ionization of La*Au* alloys illustrated in Fig. 1. Note that Fig. 1 depicts total energies for various ionized states and that we define the chemical potential for an electron at the Fermi level (E_F) as zero. The ground state in these alloys is the level with the lowest (most negative) total energy and can be approximately described as $\mathrm{La}\,3d^{10}4f^{0}\text{–}\mathrm{Au}\,5d^{10}(\mathrm{VB})^{N}$, where $(\mathrm{VB})^{N}$ represents the number of electrons in the valence band of the whole solid. In this description hybridization with $4f^{1}$ states is neglected and only the salient configurations are given, although the ground-state hybridization will be included in the numerical calculations.

Photoionization of the La*Au* system can lead to various singly ionized states, as portrayed in Fig. 1. At the lower left, the distribution seen as a result of valence-band ionization is given in which ionization of the bandlike Au $5d$ states gives prominent peaks at ~4–7 eV (see the Appendix). It is also possible to create a $3d$ core hole and it is known that two peaks are found in the XPS spectra.[1,3,26] The lowest energy is at ~832 eV above the ground state and is due to transitions to the state with the approximate configuration $\mathrm{La}\,3d^{9}4f^{1}\text{–}\mathrm{Au}\,5d^{10}(\underline{\mathrm{VB}})_{k_F}$ where $\underline{\mathrm{VB}}$ indicates a hole in the valence band and in which the core hole is "screened" by the transfer of an electron from an extended state (subscript k), labeled $(\mathrm{VB})_{k_F}$, at the Fermi level to the localized $4f$ state.[27] Note, however, that there is a continuum of other, well screened, La $3d^{9}4f^{1}$ states at slightly higher energy (Fig. 1, top left) in which the number of electrons is conserved but in which the screening $4f$ electron is taken from a valence state instead of from E_F.[28] As illustrated in Fig. 1, there is a second "poorly screened" $\mathrm{La}\,3d^{9}4f^{0}\text{–}\mathrm{Au}\,5d^{10}$ configuration at ~836 eV above the ground state, and degenerate with the $\mathrm{La}\,3d^{9}4f^{1}\text{–}\mathrm{Au}\,5d_{k}^{9}$ states in which an electron has been removed from an extended Au $5d$ state. For this paper

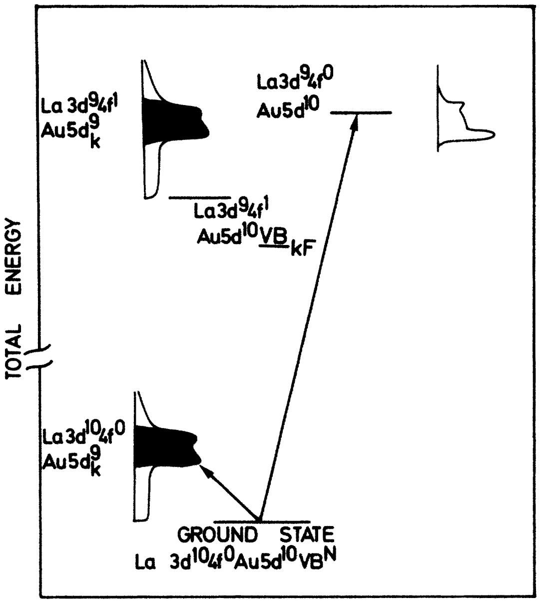

FIG. 1. Schematic diagram showing the effect of photoionization on the total energy of La*Au* alloy systems if an electron at E_F is defined to have zero chemical potential: lower left, valence-band photoemission; upper level, $3d$ ionization. The diagrams at the top left and right correspond to La $3d^9 4f^1$ and $3d^9 4f^0$ approximate local configurations (see text). The total energy of the system increases (i.e., becomes less negative) from bottom to top. Note that in the diagram the valence-band ionization processes extend all the way to the ground-state energies. We neglect the chemical potential of electrons at E_F because it is not relevant to later discussions.

the most interesting aspect of this situation is that this poorly screened state may mix, or hybridize with the La $3d^9 4f^1$–Au $5d_k^9$ continuum by a one-electron Au $5d \leftrightarrow$La $4f$ hopping process.[21] As shown schematically in Fig. 1, top right, this can lead to severe distortion of the higher-energy XPS peak, which for the sake of simplicity we continue to describe as the "poorly screened" La $3d^9 4f^0$ region.[1]

The purpose of this paper is to document virtual-bound-state broadening in the intermetallic compounds of La, Ce, Pr, and Nd with Au and to show its use as a diagnostic test of hybridization of the $4f$ levels. (Note that for Ce the above discussion still applies but the "well" and "poorly" screened states are f^1 and f^2; for Pr they are f^2 and f^3, and for Nd f^3 and f^4, respectively). We start with a description of model calculations and then present experimental results which show features which can be explained by the model. We then discuss the implications of our results for the ground state of these alloys, and also where virtual-bound-state broadening can be expected.

II. MODEL CALCULATIONS

For the purpose of the line-shape computations we must describe the situation in virtual-bound-state broadening more formally. We first give a highly simplified formalism to illustrate distortion of the *line shape* of the region we labeled poorly screened before interaction with the continuum screened states. Later a very brief description of the numerical calculations is given in which f-s hybridization is included to give the spectral *weights*.

We are interested in the line-shape distortions of the higher-energy, poorly screened component La $3d^9 4f^0$–Au $5d^{10}(\mathrm{VB})^N$ (where N is the number of electrons) due to the presence of an extra (aside from sp) structured continuum labeled at La $3d^9 4f^1$– Au $5d_k^9(\mathrm{VB})^N$. Since this continuum in the Au $5d$ band is well removed from the threshold [i.e., from the well-screened state La $3d^9 4f^1$–Au $5d^{10}(\mathrm{VB})_{k_F}^{N-1}$ with a hole in the states of largely sp character at E_F] we first treat the hybridization with the Au $5d$ states separately, neglecting the rest of the valence band. The problem to deal with is then that of a discrete state hybridizing with a structured continuum. To treat this problem we could use a basis set of final states as follows:

$$\psi_0 = |\,\mathrm{La}\,3d^9 4f^0\text{–}\mathrm{Au}\,5d^{10}\rangle \tag{1}$$

and

$$\psi_k = |\,\mathrm{La}\,3d^9 4f^1\text{–}\mathrm{Au}\,5d_k^9\rangle\ . \tag{2}$$

Upon switching on the d-f hybridization the new eigenstates would be of the form

$$\psi_n = \alpha^n \psi_0 + \sum_k \beta_k^n \psi_k \tag{3}$$

and the spectral line shape of the $3d^9 4f^0$ (ψ_0) component would be given by

$$\begin{aligned} I(\varepsilon) &= \sum_n |\langle \psi_0 | \psi_n \rangle|^2 \delta(\varepsilon + \varepsilon_f^0 - U_{fc} - \varepsilon_n - \varepsilon_c) \\ &= \sum_n |\alpha_n|^2 \delta(\varepsilon + \varepsilon_f^0 - U_{fc} - \varepsilon_n - \varepsilon_c)\ , \end{aligned} \tag{4}$$

where ε_f^0 is the $4f^1$ energy with respect to E_F in the ground state, U_{fc} is the effective $3d$-$4f$ Coulomb interaction, and ε_n and ε_c refer to the energies of the valence and core electrons.

In Eq. (4) we have neglected the hybridization between the f states and the valence states other than Au $5d$ (i.e., La spd and Au sp). Thus the total spectrum is determined by how strongly the f level mixed with the host d band in the final state. For a core hole interaction such that the f state falls within the host d band (as in Fig. 1 and LaAu$_x$) the XPS spectra will be broadened to an extent depending on the final-state f-d hybridization, V_{fd_k}. As discussed in Ref. 7, the poorly screened part of the XPS line shape in this case is given by

$$\rho_f(E) = \frac{1}{\pi} \mathrm{Im} \frac{1}{E - i0 - (\varepsilon_f^0 - U_{fc}) - \sum_k \dfrac{|V_{fd_k}|^2}{E - i0 - \varepsilon_{d_k}}}\ . \tag{5}$$

In the limit of the large f-level degeneracy (N_f) the same result is obtained, except that the factor N_f appears before the summation in the denominator of Eq.

(5). By including a sum over the valence band up to the Fermi level one would obtain the whole line shape, including the screened peaks.[7] In the limit of large N_f it is not an approximation to neglect the hybridization with states above E_F.

In our actual calculation for the La intermetallics we have included also the *sp* band, allowed for hybridization in the initial state, and taken the large degeneracy $N_f = 14$ of the f level into account. The calculation is performed to lowest order in $1/N_f$, and f^0, f^1, and f^2 configurations are taken into account.[29] If the fairly unimportant f^2 configurations are neglected an expression similar to Eq. (5) is obtained. For V_{fd_k} we assume

$$\pi \sum_k |V_{fd_k}|^2 \delta(\varepsilon-\varepsilon_k) = \frac{2V_{sf}^2}{B_s^2}(B_s^2-\varepsilon^2)^{1/2}\Theta(B_s^2-\varepsilon^2) + \frac{2V_{df}^2}{B_d^2}[B_d^2-(\varepsilon-\varepsilon_0)^2]^{1/2} \times \left[0.8+\frac{|\varepsilon-\varepsilon_0|}{5.4}\right] \times \Theta(B_d^2-\varepsilon^2)\,, \qquad (6)$$

where the first term models the *sp* band with the width $2B_s$ and the second term the d band with the width $2B_d$ taken from the experimental data of the Appendix. We use $\Delta_{fd} = 2V_{df}^2/B_d$ or $\Delta_{fs} = 2V_{sf}^2/B_s$ as measures of the strength of the coupling to the d band or the *sp* and La $4d$ band, respectively. Δ_{fs} is 38 meV here.

For our calculations we take the position of the bare $4f$ level in the final state (i.e., the separation of the $\underline{c}4f^{n+1}$ and $\underline{c}4f^n$ thresholds where $\underline{c}$ represents core holes) to be 5.0 eV, which is roughly the average for the first four rare earths. The results are plotted in Fig. 2 after broadening with a 1.8-eV full width at half maximum (FWHM) Lorentzian function to compare with experiment[30] and with a 0.1-eV FWHM Lorentzian to illustrate the underlying effects more clearly. The curves with 0.1-eV broadening show a tendency to split off two peaks at the top and bottom of the d band. For $\Delta_{fd} = 36$ meV the coupling is not strong enough to give any appreciable structure at the bottom of the band but already large enough to give a non-Lorentzian contribution. For $\Delta_{fd} = 57$ meV we already have the peaks at the top and bottom of the band but there is a lot of weight in between. As Δ_{fd} is increased, weight is transferred to the band edges and for $\Delta_{fd} = 145$ meV the peaks at the band edges dominate.

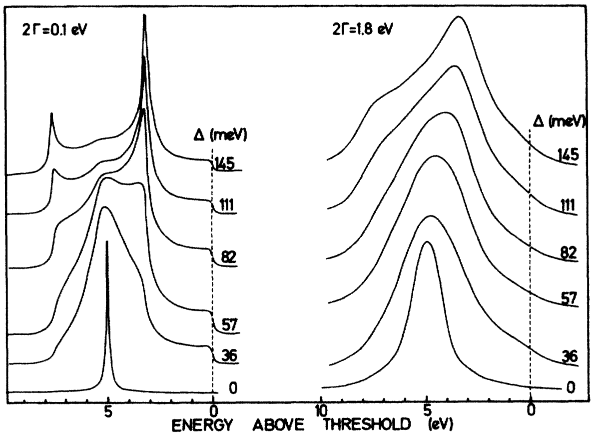

FIG. 2. Simulations of the $3d^9 4f^n$ XPS line shapes in the absence of $3d^9 4f^n$ or $3d^9 4f^{n+1}$ multiplet splitting. The Δ in the figures gives the value Δ_{df}. Δ_{sf} was chosen to be 38 meV, B_s was 8 eV, and a B_d of 2.2 eV was chosen as appropriate for $LaAu_2$ (see the Appendix).

If we use a large broadening of 1.8 eV, comparable to the sum of lifetime and experimental broadening, the structure is washed out and the transfer of weight to the d-band edges looks like an increase in the peak width. It is quite important to recognize that there is no simple and general relationship between observable peak width and the d-f hybridization. For instance, if V_{df} is held constant at a value which gives $\Delta_{fd} \sim 60$ meV in $LaAu_2$, but the d-band width is decreased, then Δ_{fd} increases. However, the XPS peak will actually narrow because of the smaller separation of the peaks at the d-band edges.

III. EXPERIMENT

The samples were prepared by melting appropriate quantities of the elements in a cold crucible. They were characterized by metallographic methods and by x-ray diffraction and shown to contain less than 5% of second phases. The samples were cleaned by scraping with an Al_2O_3 file and their XPS spectra measured in a vacuum of typically 5×10^{-11} torr using monochromated Al $K\alpha$ radiation. Total instrumental resolution was about 0.65 eV.

IV. RESULTS

Two illustrations of the influence of virtual-bound-state broadening are given in Figs. 3 and 4. In Fig. 3 we

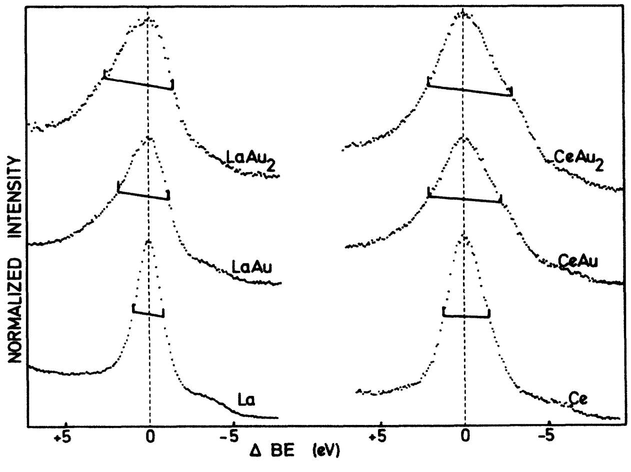

FIG. 3. The measured $3d_{5/2}^9$ XPS line shapes of La, LaAu, $LaAu_2$, and their Ce analogues.

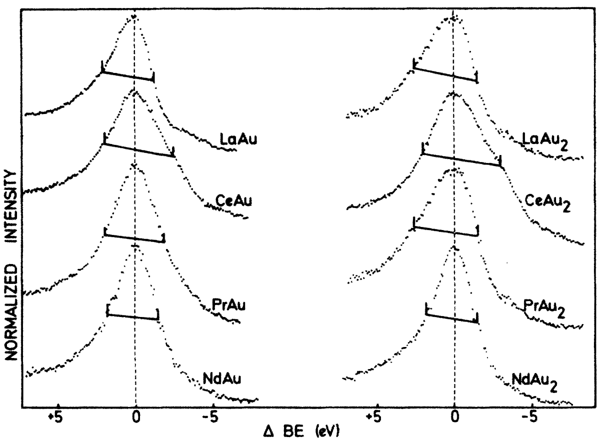

FIG. 4. $3d^9_{5/2}$ XPS peaks of the 1:1 and 1:2 alloys of La, Ce, Pr, and Nd with Au.

plot the XPS spectra of La, LaAu, LaAu$_2$, and the Ce analogues. The well-screened f^1 peak of La and f^2 peak of Ce are a small step ~4–6 eV below the main peak. Note that the La and Ce $3d$ peaks are significantly broader in the Au intermetallic compounds. The peak shapes are found on detailed examination to be complex; they are not simple broadened peaks but often exhibit what seem to be partly resolved shoulders. We found broadened peaks in many of the alloys of La and Ce we studied. In general the order of the observed peak widths was $w(M) \sim w(M\mathrm{Al}_x) \sim w(M\mathrm{Se}) < w(M\mathrm{Ni}) < w(M\mathrm{Pd}) < w(M\mathrm{Au})$ (where M represents a rare earth), which is approximately the order of the density of electronic states 3–5 eV below E_F.

In Fig. 4 the $3d_{5/2}$ XPS peaks are compared for the 1:1 and 1:2 intermetallic compounds of rare earths with Au. The peaks are again seen to have complex shapes, especially in Ce, and the widths are smaller for Nd than for Ce.

V. DISCUSSION

A. Assignment of the observed broadening

Virtual-bound-state broadening is an explanation which fits the experimental facts. Secondary phases and contamination are absent, and in any case would be distinguished by other features in the spectrum. Multiplet effects due to the interaction between the $4f$ and between the $4f$ and $3d$ electrons are absent in the La $4f^0$ peaks and in Ce, Pr, and Nd they are present in the pure elements as well as the alloys. In any case these effects are stronger in Nd than in La or Ce, while the opposite is true of the observed broadening. Further, the virtual-bound-state broadening mechanism can qualitatively explain the observed $\underline{c}4f^n$ peak widths in La and Ce alloys which increase in the order $w(\mathrm{Al}) \sim w(\mathrm{Se}) < w(\mathrm{Ni}) < w(\mathrm{Pd}) < w(\mathrm{Au})$.

B. The size of the 4*f* hybridization and the strength of the observed effects

Figures 2–4 illustrated the sensitivity of the $\underline{c}4f^n$ peaks to the strength of hybridization, Δ, between the $\underline{c}4f^n$ level and the $\underline{c}4f^{n+1}\,\underline{k}$ continuum (where $\underline{k}$ is a state in k space). In principle then, one should be able to determine Δ from the peak shape. Unfortunately this peak shape is also sensitive to the precise details of the valence-band density of states and the sizes of the $\underline{c}4f^n$ and $\underline{c}4f^{n+1}$ threshold separations relative to the position of the principle features in the density of valence-band states. The $\underline{c}4f^n$ and $\underline{c}4f^{n+1}$ multiplet structures should also be taken into account. All of these details make a true "fit" of model parameters to simulate the spectra impractical and of value not commensurate with the work involved. However, simulations such as those given in Fig. 2 convince us that virtual-bound-state broadening is compatible with all of the nuances of the observed spectra if Δ_{fd} is taken to be ~100 meV in LaAu$_x$ and CeAu$_x$. In PrAu$_x$ and NdAu$_x$ the hybridization will be smaller and the virtual-bound-state broadening is further decreased by the degeneracy changes. The narrowness of the La peaks with respect to Ce in their Au intermetallics is not attributed to a change in Δ_{fd}, but to the fact that the $\underline{c}4f^n$:$\underline{c}4f^{n+1}$ threshold separation is lower in La (~4 eV) so that most of the spectral weight occurs at the top of the features dominated by the Au $5d$ states: in Ce the threshold separation (~4.6 eV) is such as to shift weight to both wings of the peak.

C. The relationship between the Δ measured by virtual-bound-state broadening and the $\underline{c}f^n$:$\underline{c}f^{n+1}$ peak intensity ratios

In a system with screening orbitals it is well known that the ratio of intensities in the well and poorly screened peaks (i.e., $4f^n$ and $4f^{n+1}$ XPS peaks with screening orbital predominantly occupied and empty, respectively) depends on the hybridization of the screening orbital with the valence states. In recent years much work has been done to extract data on the hybridization between the $4f$ level and the valence states using this effect [intensity ratio method (I)]. In this context it is notable that the values of Δ_{fd} found by the virtual-bound-state method *are* comparable to the values for $4f$ hybridization with the $4d$ and $5d$ bands in MPd$_x$ and MPt$_x$ compounds by the intensities method.[8,11]

For LaAu and LaAu$_2$ we have earlier obtained $\Delta \sim 30$ meV using this method and assuming a relatively structureless band.[8,11] In the intensity method the states within a few eV of E_F play a particularly important role, and for LaAu$_x$ the intensity method therefore gives information mainly about the coupling to the La *spd* and Au *sp* bands. The quoted value of 30 meV is therefore in fair agreement with $\Delta_{fs} = 38$ meV obtained here from a more careful fit to the weight of the f^1 shoulder. We note that the two methods are complementary in that the intensity and virtual-bound-state broadening methods primarily give information about the coupling to the states within a few eV of E_F and about 5 eV below E_F, respectively.

D. Relevance of these results to valence-band photoemission

It is clear from our results that hybridization between the $\underline{c}4f^{n+1}\ \underline{k}$ threshold and the $\underline{c}4f^{n}$ continuum can broaden and distort the shape of a core-level line. This being the case, it is clear that when a $4f$ electron is removed in valence-band photoemission there will be a comparable effect on the line shape due to interaction between the $4f^{N-1}$ threshold and the $4f^{n}(\mathrm{VB})^{N-1}$ states. This leads to broadening and distortion of the $4f^{n-1}$ lines when their binding energy overlaps the matrix valence-band states. Clear examples of such shape distortion are evident in photoemission studies of Mn, Pd, and Pt impurities in Cu and Ag.[18–20] Also in the resonance valence-band photoemission spectra of light rare-earth intermetallics the $4f$ contributions to the spectra exhibit complex shapes,[31,32] which have sometimes been interpreted in terms of overlapping Lorentzians. However, such complex shapes may also be attributed to non-Lorentzian distortion of the $4f$ "virtual bound states," as documented quantitatively elsewhere.[33]

VI. CONCLUDING REMARKS

We have discussed (non-Lorentzian) distortion of core-level line shapes by virtual-bound-state-like broadening which arises because the state from which an electron hops into a localized screening orbital from the full valence states is degenerate with the energy of a poorly screened state. We have given a model calculation to illustrate the physics of this process, and shown that such effects are strong in XPS spectra of early rare-earth atoms in intermetallic compounds with gold and other elements. These effects can in principle be used to measure directly the strength of hybridization between localized orbitals and the valence states.

The virtual-bound-state-like broadening is not restricted to XPS. As mentioned before it is known in Auger spectroscopy. A description has already been given for Ni L_3VV spectra in Ni alloys.[22] As another example we note that in Ag-Pd alloys the Pd $M_{4,5}N_{4,5}N_{4,5}$ transition leads to a Pd $4d^8$ final state which is degenerate with a Pd $4d^9$-Ag $4d^9$ state; i.e., one of the two Pd $4d$ holes can hop onto a Ag site.[24,25,34] We also expect similar effects in some XAS spectra. Consider, for instance, the $M_{4,5}$ ($3d$) and L_3 ($2_{p_{3/2}}$) absorption edges of Ce and its compounds. The main transition in the $3d$ spectra is $3d \rightarrow 4f$ so that most of the weight is found in transitions to the $\underline{c}4f^{n+1}$ states, which are the lowest-lying core-ionized states and show no virtual-bound-state broadening. This is not the case for the $2p$ edges of rare earths in which the main transitions are $p \rightarrow d$ and the spectra are dominated by transitions to $\underline{c}4f^{n}$ final states, which are not the lowest-lying core-ionized states. Effects are difficult to observe here because of the poorer resolution and larger intrinsic lifetime broadening of the core level, and the width due to the Ce unoccupied $5d$ bandwidth. However, in principle virtual-bound-state broadening should be observable for the same compounds for which it is observed in the Ce $3d$ XPS spectra.

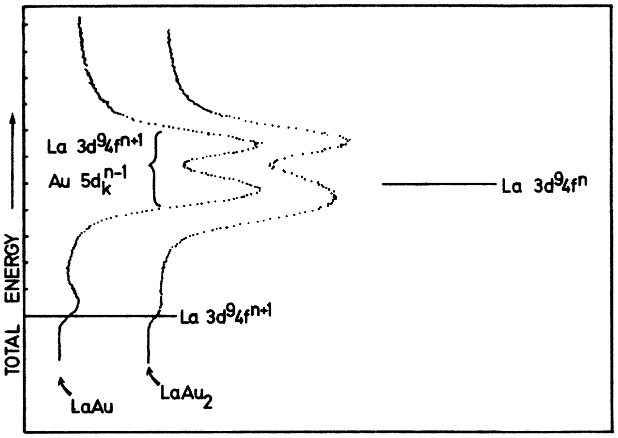

FIG. 5. XPS valence-band spectra of LaAu and $\mathrm{LaAu_2}$.

ACKNOWLEDGMENTS

Experimental data were obtained in the Kernforschungsanlage Jülich. We thank M. Beyss, J. Keppels, and J.-M. Welter for technical assistance and M. Campagna for his support and stimulating discussions. This work has been supported in part by the organizations Scheikundig Onderzoek Nederland and Fundamenteel Onderzoek der Materie with financial support of the Dutch organization for support of pure science (ZWO). We also acknowledge a North Atlantic Treaty Organization (NATO) travel grant which made cooperation between the authors possible.

APPENDIX

The valence-band XPS spectra of LaAu and $\mathrm{LaAu_2}$ are presented in Fig. 5. Such XPS spectra are normally presented with the intensity as a function binding energy relative to E_F. Here, to be consistent with Fig. 1 and to illustrate the influence of the valence-band structure we show the spectra in conjunction with the relative positions of the La $3d^9 4f^{n+1}$ and La $3d^9 4f^{n}$ threshold states.

The XPS valence-band spectra are dominated by the Au $5d$ states which are much narrower than in pure Au. For LaAu the approximate $5d$ bandwidth after correction for instrumental resolution is ~ 3 eV and the peaks are found at ~ 4.8 and ~ 6.4 eV. The centroid is at ~ 5.5 eV. For $\mathrm{LaAu_2}$ the Au $5d$ peaks are at ~ 4.6 and ~ 6.7 eV with the centroid at ~ 5.4 eV and the width ~ 4 eV.

[1] J. C. Fuggle, M. Campagna, Z. Zołnierek, R. Lässer, and A. Platau, Phys. Rev. Lett. **45**, 1597 (1980).

[2] G. Krill, J. P. Kappler, A. Meyer, L. Abadli, and M. F. Ravet, J. Phys. F **11**, 1713 (1981).

[3] S.-J. Oh and S. Doniach, Phys. Rev. B **26**, 2085 (1982).

[4] J. W. Allen and R. M. Martin, Phys. Rev. Lett. **49**, 1106 (1982).

[5] N. Mårtensson, B. Reihl, and R. D. Parks, Solid State Commun. **41**, 573 (1982).

[6] O. Gunnarsson and K. Schönhammer, Phys. Rev. Lett. **50**, 604 (1983).

[7] O. Gunnarsson and K. Schönhammer, Phys. Rev. B **28**, 4315 (1983).

[8] J. C. Fuggle, F. U. Hillebrecht, Z. Zołnierek, R. Lässer, Ch. Freiburg, O. Gunnarsson, and K. Schönhammer, Phys. Rev. B **27**, 7330 (1983).

[9] O. Gunnarsson, K. Schönhammer, J. C. Fuggle, F. U. Hillebrecht, J.-M. Esteva, R. C. Karnatak, and B. Hillebrand, Phys. Rev. B **28**, 7330 (1983).

[10] E. Wuilloud, H. R. Moser, W.-D. Schneider, and Y. Baer, Phys. Rev. B **28**, 7354 (1983).

[11] J. C. Fuggle, Physica **130B**, 56 (1985), and references therein.

[12] O. Gunnarsson and K. Schönhammer, J. Magn. Magn. Mater. **52**, 141 (1985), and references therein.

[13] J. C. Fuggle, E. Umbach, D. Menzel, K. Wandelt, and C. R. Brundle, Solid State Commun. **27**, 65 (1978).

[14] O. Gunnarsson and K. Schönhammer, Phys. Rev. Lett. **41**, 1608 (1978); Z. Phys. B **30**, 297 (1978).

[15] E. Umbach, Surf. Sci. **117**, 482 (1982), and references therein.

[16] E. Umbach, Solid State Commun. **51**, 365 (1984).

[17] Very preliminary reports of this effect have also been given elsewhere for Ce systems, see J. C. Fuggle, *X-Ray and Atomic Inner-Shell Physics (University of Oregon, Eugene, Oregon)*, Proceedings of the International Conference on X-Ray and Atomic Inner-Shell Physics—1982, AIP Conf. Proc. No. 94, edited by B. Crasemann (AIP, New York, 1982).

[18] D. v. d. Marel, G. A. Sawatzky, and J. A. Julianus, J. Phys. F **14**, 281 (1984).

[19] A. Bosch, H. Feil, G. A. Sawatzky, and J. A. Julianus, J. Phys. F **14**, 2225 (1984).

[20] D. v. d. Marel, G. A. Sawatzky, and F. U. Hillebrecht, Phys. Rev. Lett. **53**, 206 (1984).

[21] In solid-state physics it is common to encounter a localized impurity state below the bottom of the valence band which is called a "bound state." It is also possible to find highly localized impurity states within the band, which are called virtual-bound states. In so far as the Anderson impurity model can be applied to the rare-earth $4f$ levels, these may also be described as virtual bound states.

[22] P. A. Bennett, J. C. Fuggle, F. U. Hillebrecht, A. Lenselink, and G. A. Sawatzky, Phys. Rev. B **27**, 2194 (1983).

[23] M. Vos, G. A. Sawatzky, M. Davies, P. Weightman, and P. T. Andrews, Solid State Commun. **52**, 159 (1984).

[24] P. Hedegård and B. Johansson, Phys. Rev. Lett. **52**, 2168 (1984).

[25] M. Vos, D. v. d. Marel, and G. A. Sawatzky, Phys. Rev. B **24**, 3037 (1984).

[26] G. K. Wertheim and M. Campagna, Solid State Commun. **26**, 553 (1978); G. Crecelius, G. K. Wertheim, and D. N. E. Buchanan, Phys. Rev. B **18**, 6519 (1978).

[27] The states are not "pure" $4f^n$ or $4f^{n+1}$ due to hybridization of the $4f$ levels with the valence states. Note also the interactions between the $4f$ electrons and the core hole lead to multiplet fine structure which is of secondary importance here.

[28] In fact, each of the states mentioned has further continua associated with it which are formed by creation of an electron-hole pair with an electron being excited to any of the states above E_F. The coupling of our system to these states is via higher-order terms and is weaker than the effects we discuss.

[29] In principle one must include not only the continuum with one electron-hole pair in the valence band, $f^n\ (e\text{-}h)$, but higher continua with multiple electron-hole pairs, $f^n\ (e\text{-}h)^x$, but in both experiment and theory the former seem most important. In theoretical studies one e-h pair gives nearly the correct result for a nondegenerate f level and if N_f is large the e-h pairs are even less important (Ref. 7).

[30] 1.8 eV is probably too large to simulate the La $3d_{5/2}$ spectra where the instrumental broadening is only ~0.65 eV and lifetime broadening seems to be only 0.4–0.8 eV [B. T. Thole, G. v. d. Laan, J. C. Fuggle, G. A. Sawatzky, R. C. Karnatak, and J.-M. Esteva, Phys. Rev. B **32**, 5107 (1985)]. It is more suitable for Ce where multiplet effects give an additional broadening contribution.

[31] R. D. Parks, S. Raaen, M. L. den Boer, Y. S. Chaug, and G. P. Williams, Phys. Rev. Lett. **52**, 2176 (1984).

[32] G. Kalkowski, E. V. Sampathkumaran, C. Laubschat, M. Domcke, and G. Kaindl, Solid State Commun. **55**, 977 (1985).

[33] J. W. Allen, S. J. Oh, O. Gunnarsson, K. Schönhammer, M. B. Maple, M. S. Torikachvili, and I. Lindau, Adv. Phys. **35**, 275 (1985).

[34] M. Vos, G. A. Sawatzky, M. Davies, P. Weightman, and P. T. Andrews, Solid State Commun. **52**, 159 (1984).